

Observation of Postcollision Effects in the Scattered Projectile Spectra for Ionizing Proton-Helium Collisions

T. Vajnai,* A. D. Gaus, J. A. Brand, W. Htwe,[†] D. H. Madison, R. E. Olson, J. L. Peacher, and M. Schulz

Department of Physics and the Laboratory for Atomic and Molecular Research, University of Missouri-Rolla, Rolla, Missouri 65401

(Received 28 July 1994)

We have measured and calculated doubly differential single ionization cross sections as a function of the scattering angle and the projectile energy loss for 50 to 150 keV proton-helium collisions. These cross sections show unexpected structures as a function of both the energy loss and the scattering angle, which are interpreted as due to the postcollision interaction. Although the effects of postcollision interactions have previously been observed in electron spectra, this is the first observation of such effects for the scattered protons.

PACS numbers: 34.50.Bw, 34.50.Fa

One advantage of studying atomic collision processes is that the underlying fundamental force, the electromagnetic force, is well understood. However, our understanding of the dynamics of the interactions is still incomplete. One major problem is that the Schrödinger equation is not solvable for more than two bodies without using approximations. Furthermore, the long-range nature of the Coulomb force gives rise to several difficulties in the applications of the formal collision theory. The development of the theory indicates that, for example, a satisfactory description of ion-induced ionization requires the proper representation of the asymptotic three-body Coulomb wave functions, which are unknown [1] except for some special cases. The ionized electron experiences the field of both the target nucleus and the outgoing projectile even after traveling a long distance from the collision region. This interaction of the ejected electron after the actual ionization process is called the postcollision interaction (PCI). A prominent example of the effect of the PCI is electron capture to the continuum (ECC). In the ECC process an electron is transferred from a bound target state to a low-lying continuum state of the projectile, resulting in the so-called “cusp” peak in the energy spectrum of the forward ejected electrons at electron velocities v_e equal to the velocity of the projectile v_p . The theories for electron emission in the forward direction have to take into account the interaction between the proton and the electron in the final state [2,3]. Salin [2] introduced a distortion of the final-state wave function for the outgoing electron due to the projectile using the first-order Born approximation.

Since the pioneering experiments of Crooks and Rudd [4] and Harrison and Lucas [5], who measured the full angular and energy distributions of ionized electrons in collisions of protons with helium [4] and thin foils [5], PCI effects have been the subject of numerous experimental and theoretical investigations [6–18]. Most of these studies focused on the effect of the PCI on the electron’s angular and energy distributions. It was commonly held that

cusp electrons only make an important contribution to the ionization cross section for electron emission angles of 0° and that they are insignificant in the cross sections integrated over all electron angles. Very little work has been performed on studying the effect of the PCI on the scattered projectiles. From momentum conservation considerations, some effect on the projectile would be expected to counterbalance the effect on the electron. However, because of the large projectile to electron mass ratio, the effect on the projectile would not be expected to be as pronounced as on the electron. To the best of our knowledge no evidence for an observable effect of the PCI on outgoing heavy projectiles has been reported.

In this Letter we report the first evidence that the angular distribution of heavy scattered projectiles can be significantly influenced by the postcollision interaction. Furthermore, our studies indicate that cusp electrons can significantly affect the heavy particle differential ionization cross sections even after integrating over all electron angles.

This experiment was performed on the University of Missouri-Rolla Ion Energy-Loss Spectrometer (UMRIELS). Details of the apparatus and method are described elsewhere [19,20] and are only briefly summarized here. A proton beam was obtained from a hot cathode ion source with a narrow energy spread (<1 eV) and accelerated to energies ranging from 50 to 150 keV. The beam was collimated and steered into a target gas cell containing helium at a pressure of 50 mTorr over a length of 1 cm. The beam was then cleaned from charge-changed components by a switching magnet. After the magnet the protons passed through a solid angle defining collimator. The angular resolution was $75 \mu\text{rad}$. Finally, the protons were decelerated to an energy of 2 keV and energy analyzed by a parallel plate analyzer. The energy loss was set by applying an offset voltage to the accelerator relative to the decelerator potential. Only the protons which suffered an energy loss equal to the offset voltage would be decelerated to the pass energy

of the analyzer. The overall energy resolution was 1.5 eV full width at half maximum (FWHM). The angular profile of the scattered beam at a fixed energy loss was obtained by pivoting the accelerator around the center of the target chamber. Data were taken for scattering to both sides of the incident beam direction. The measurements were then repeated for energy losses ranging from 25 to 150 eV. An angular profile was also taken for the incident beam (zero energy loss) with the target gas taken out and was later used to deconvolute the divergence of the beam from the measured angular distribution of the protons suffering specific energy losses [20]. A pressure dependence of the projectile count rate was taken to ensure single collision conditions.

In Fig. 1(a) we show a three-dimensional plot of the doubly differential single ionization cross sections as a function of the ionized electron energy and the projectile scattering angle for a collision energy of 50 keV. The electron energy is obtained by subtracting the He ionization potential from the energy loss. The cross sections are presented on a relative scale. Absolute cross sections were determined and will be reported in a forthcoming paper. Here, we focus on the shape of the cross sections as a function of the electron energy and the projectile scattering angle.

The characteristics of the cross sections are typical for most inelastic processes: The cross sections drop with both increasing electron energy and increasing scattering angle. However, apart from this general trend, there is a pronounced shoulder at an electron energy around 25 eV. This shoulder becomes less pronounced with increasing scattering angle as is shown in the equal angle contour lines. The electron energy where the shoulder occurs corresponds to electrons moving at the same velocity as the projectile. The same effect was observed for all measured collision energies: In each case a shoulder was found near an electron energy $E_e = (m_e/M)E_0$ corresponding to an electron having the same velocity as the projectile (matching velocity), where m_e/M is the electron to projectile mass ratio and E_0 is the collision energy.

The three-dimensional plots in Figs. 1(b) and 1(c) show calculated doubly differential cross sections as a function of the electron energy and the projectile scattering angle. Figure 1(b) shows a plane wave Born approximation (PWBA) calculation. This calculation only includes the projectile-electron interaction to first order and no PCI effects are taken into account. For this calculation, no structure is observed near the matching velocity at any collision energy. Figure 1(c) also shows a plane wave Born calculation; however, here the PCI is taken into account following the method of Salin [2]. This calculation shows very similar features to our experimental data: At all collision energies a shoulder is found near the matching velocity. It should be noted that the irregularities in the constant angle contour lines are an artifact of the plotting software.

The important features of the three-dimensional plots of the experimental and theoretical cross sections can be summarized in two points: (1) The experimental data always show a structure near the matching velocity, which corresponds to the same energy at which cusp electrons were observed in electron spectra in the forward direction. (2) In the calculations these structures are only obtained if the PCI is taken into account. Furthermore, we note that cusp electrons are a manifestation of PCI effects. Combining these observations, we infer that the shoulder near the matching velocity is due to the same mechanism as that leading to the cusp peaks in the electron spectra. This means that the contribution of cusp electrons to the cross sections differential in heavy projectile scattering angle and energy is significant near the matching velocity even though these cross sections are integrated over all electron angles.

In order to study the influence of the PCI on the scattering angular distribution of the projectiles, we have analyzed the cross sections for fixed electron energies as a function of projectile scattering angle. We have determined the widths of the measured angular distributions (both sides from the incident beam direction) by fitting them with a combination of a Gaussian and a Lorentzian function. This particular combination was chosen merely

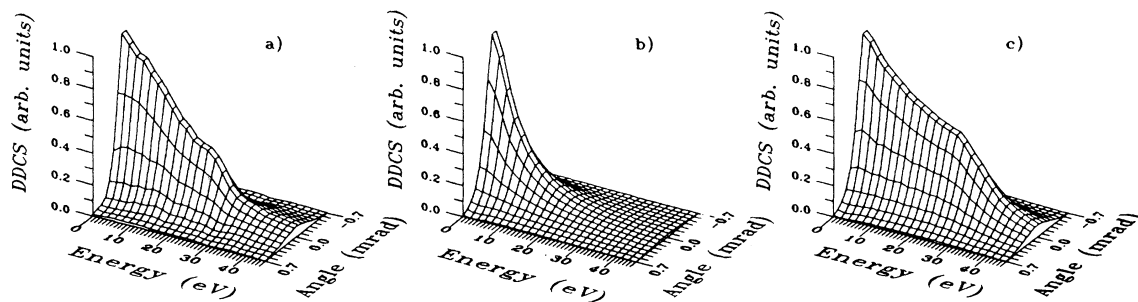


FIG. 1. Doubly differential single ionization cross sections for 50 keV $p + \text{He}$ collisions as a function of the ionized electron energy and the projectile scattering angle. (a) The experimental data; (b) the PWBA calculation without the PCI; (c) the PWBA calculation with the PCI.

because it was found to give a very good fit to the data and should thus provide reliable widths. The half widths at half maximum obtained from this fit are plotted as closed symbols in Fig. 2 for all collision energies as a function of the ratio of the electron velocity to the projectile velocity. The measurements were repeated several times and the widths could be reproduced within $10 \mu\text{rad}$ so that the uncertainties are typically not significantly larger than the size of the data points. The dashed curves show the widths obtained from the PWBA calculation without the PCI, the full curves are the PWBA calculations with the PCI, and the open symbols show four-body classical trajectory Monte Carlo (CTMC) calculations. It should be noted that the PCI is inherently included in the CTMC calculations, which have previously been shown to reproduce both the shape and the magnitude of the cusp electron spectra at 50 and 100 keV $p + \text{He}$ collisions [21].

The general trend of the experimental data of Fig. 2 follows what one might expect: Since an increasing energy transfer to the electron requires an increasingly closer collision with the electron, the angular width of the cross sections tends to increase with increasing electron velocity. However, a closer inspection of the

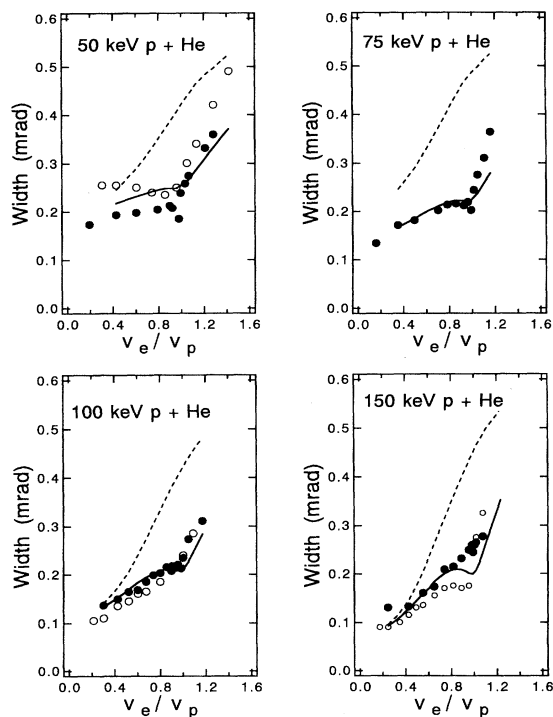


FIG. 2. Widths of the angular distribution of the doubly differential single ionization cross sections as a function of the ratio of the electron velocity to the projectile velocity. The closed symbols are our experimental data, the open symbols are the CTMC calculations, the dashed curves represent the PWBA calculations without the PCI, and the solid curves the PWBA calculations with the PCI.

data shows some surprising features. The data follow the expected trend until the electron velocity is near the matching velocity. Here, a distinct change of the slope is observed and the widths increase much more steeply after the matching velocity. This effect is particularly pronounced for collision energies of 50 and 75 keV. It is much less noticeable for 100 keV and is not observed in the experimental data for 150 keV. This distinct change of slope is also found in our calculations including the PCI. Furthermore, the PWBA calculation including the PCI consistently predicts a minimum in the widths at the matching velocity, whereas the PWBA calculation without the PCI monotonically increases without any structure or change of slope near the matching velocity. The CTMC calculations for 50 and 150 keV also show a minimum and a subsequent change of slope near the matching velocity. Both the CTMC calculation and the PWBA calculation including the PCI are in reasonably good agreement with the experimental data, except for 150 keV around the matching velocity, where both calculations underestimate the widths. The PWBA calculation without the PCI drastically overestimates the widths with the largest discrepancy occurring at the matching velocity.

The observed change of slope in the width as a function of electron velocity can be explained qualitatively in terms of the PCI. Because of the PCI the ionized electron and the outgoing projectile attract each other towards the incident beam direction. This "focusing effect" tends to make the scattering angular distribution of the cross sections narrower. Furthermore, the focusing effect should depend sensitively on the relative velocity between the electron and the projectile. It should maximize around the matching velocity, where the average relative velocity minimizes. Therefore, below the matching velocity, the focusing effect becomes increasingly important with increasing electron velocity, which would tend to decrease the angular width. On the other hand, an increasing energy transfer to the electron requires increasingly closer collisions. This tends to broaden the angular distribution as mentioned above. The combination of these two effects (counteracting each other) leads to a relatively flat dependence of the widths on the electron velocity below the matching velocity (in the calculation the focusing effect becomes dominant near the matching velocity leading to the minima). At electron velocities above the matching velocity, the focusing effect due to the PCI should be approximately the same as below the matching velocity for equal relative velocities. However, here an increasing electron velocity means an increasing relative velocity so that the focusing effect becomes less important with increasing electron velocity. Therefore, both effects tend to lead to a broader angular distribution with increasing electron velocity. Consequently, the slope of the widths as a function of electron velocity increases significantly for electron velocities above the matching velocity. We

would expect the focusing effect to become insignificant for very high electron velocities. Indeed, for electron velocities larger than twice the matching velocity the PWBA calculations with and without PCI are identical to within less than 10%.

Our PWBA calculation with the PCI indicate a stronger effect as the projectile energy increases. This is in opposition to the data which suggest that the focusing effect becomes increasingly more important for decreasing projectile energies. In the CTMC calculation, on the other hand, the focusing effect is most pronounced (strongest minimum in the width) at 50 keV and it seems to minimize at a projectile energy of about 100 keV. These differences in the projectile energy dependences of our data and calculations are currently not understood and more theoretical work on this question is needed.

One advantage of the CTMC calculation over the PWBA calculations is that it takes the interaction of the projectile with the target nucleus into account. In the PWBA calculations the projectile only gets deflected by the interaction with the target electron. At the larger scattering angles we expect the deflection of the projectile to be dominated by the interaction of the projectile with the target nucleus. On the other hand, at scattering angles smaller than 0.5 mrad the angular shape of our measured cross sections is well reproduced by the PWBA calculation with PCI. Since the widths shown in Fig. 2 are much smaller than 0.5 mrad in all cases, we do not believe that our analysis of the PCI is significantly affected by the projectile-target nucleus interaction. However, a quantitative description of the ionization cross sections, especially at larger scattering angles, will require a proper incorporation of this interaction.

In summary, we have measured and calculated $p + \text{He}$ ionization cross sections doubly differential in the projectile scattering angle and energy. We have for the first time observed the effect of the PCI on the angular deflection and energy loss of the projectile, contrary to previous expectations. We found that cusp electrons can make an important contribution to the doubly differential single ionization cross sections even after integrating over the ionized electron angular distribution. Our data provide an important test case for the proper description of the asymptotic Coulomb wave functions in theoretical calculations. The correct treatment of the asymptotic Coulomb wave function is not only important for ionization processes, but it is of general relevance in collision phenomena because other reaction channels can be coupled to the continuum.

This work was supported by National Science Foundation Grants No. PHY 9020813 and No. PHY 9116199 and by the Office of Fusion Energy, Department of Energy.

*Present address: Department of Physics, University of Miskolc, 3515 Miskolc, Hungary.

†Present address: Division of Arts and Sciences, Spoon River College, Canton, Illinois 61520.

- [1] J. H. McGuire, T. Reeves, N. C. Deb, and N. C. Sil, Nucl. Instrum. Methods Phys. Res., Sect. B **24/25**, 243 (1987).
- [2] A. Salin, J. Phys. B **2**, 631 (1969).
- [3] J. Macek, Phys. Rev. A **1**, 235 (1970).
- [4] G. B. Crooks and M. E. Rudd, Phys. Rev. Lett. **25**, 1599 (1970).
- [5] K. G. Harrison and M. W. Lucas, Phys. Lett. **33A**, 142 (1970).
- [6] R. Shakeshaft and L. Spruch, Phys. Rev. Lett. **41**, 1037 (1978).
- [7] W. Meckbach, I. B. Nemirovsky, and C. R. Garibotti, Phys. Rev. A **24**, 1793 (1981).
- [8] W. Meckbach, P. J. Focke, A. R. Göni, S. Suárez, J. Macek, and M. G. Menendez, Phys. Rev. Lett. **57**, 1587 (1986).
- [9] G. C. Bernardi, S. Suárez, P. D. Fainstein, C. R. Garibotti, W. Meckbach, and P. Focke, Phys. Rev. A **40**, 6836 (1989).
- [10] R. E. Olson, Phys. Rev. A **27**, 1871 (1983).
- [11] R. E. Olson, T. J. Gay, H. G. Berry, E. B. Hall, and V. D. Irby, Phys. Rev. Lett. **59**, 36 (1987).
- [12] T. J. Gay, H. G. Berry, E. B. Hale, V. D. Irby, and R. E. Olson, Nucl. Instrum. Methods Phys. Res., Sect. B **31**, 336 (1988).
- [13] T. J. Gay, M. W. Gealy, and M. E. Rudd, J. Phys. B **23**, L823 (1990).
- [14] W. Meckbach, S. Suárez, P. Focke, and G. Bernardi, J. Phys. B **24**, 3763 (1991).
- [15] R. D. DuBois, Phys. Rev. A **48**, 1123 (1993).
- [16] L. Sarkadi, J. Pálinkás, Á. Kövér, D. Berényi, and T. Vajnai, Phys. Rev. Lett. **62**, 527 (1989).
- [17] S. Suárez, C. Garibotti, W. Meckbach, and G. Bernardi, Phys. Rev. Lett. **70**, 418 (1993).
- [18] O. Jagutzki, R. Koch, A. Skutlarz, C. Kelbch, and H. Schmidt-Böcking, J. Phys. B **24**, 993 (1991).
- [19] J. T. Park, in *Collision Spectroscopy*, edited by R. G. Cooks (Plenum, New York, 1978), p. 19.
- [20] J. T. Park, J. M. George, J. L. Peacher, and J. E. Aldag, Phys. Rev. A **18**, 48 (1978).
- [21] C. O. Reinhold and R. E. Olson, Phys. Rev. A **39**, 3861 (1989).